2D Materials

PAPER

Magnetic field mixing and splitting of bright and dark excitons in monolayer $MoSe_2$

To cite this article: Zhengguang Lu *et al* 2020 *2D Mater.* **7** 015017

2D Materials

RECEIVED
9 October 2019

ACCEPTED FOR PUBLICATION
11 November 2019

PUBLISHED
21 November 2019

PAPER

Magnetic field mixing and splitting of bright and dark excitons in monolayer $MoSe_2$

Zhengguang Lu[1,2], Daniel Rhodes[3], Zhipeng Li[4,5], Dinh Van Tuan[6], Yuxuan Jiang[1], Jonathan Ludwig[1,2], Zhigang Jiang[8], Zhen Lian[4], Su-Fei Shi[4], James Hone[3], Hanan Dery[6,7] and Dmitry Smirnov[1]

[1] National High Magnetic Field Laboratory, Tallahassee, FL 32310, United States of America
[2] Department of Physics, Florida State University, Tallahassee, FL 32306, United States of America
[3] Department of Mechanical Engineering, Columbia University, New York, NY 10027, United States of America
[4] Department of Chemical and Biological Engineering, Rensselaer Polytechnic Institute, Troy, NY 12180, United States of America
[5] School of Chemistry and Chemical Engineering, Shanghai Jiao Tong University, Shanghai, 200240, People's Republic of China
[6] Department of Electrical and Computer Engineering, University of Rochester, Rochester, NY 14627, United States of America
[7] Department of Physics and Astronomy, University of Rochester, Rochester, NY 14627, United States of America
[8] School of Physics, Georgia Institute of Technology, Atlanta, GA 30332, United States of America

E-mail: smirnov@magnet.fsu.edu

Keywords: two-dimensional materials, transition metal dichalcogenide monolayers, molybdenum diselenide, dark excitons, electronic and optical properties

Supplementary material for this article is available online

Abstract

Monolayers of semiconducting transition metal dichalcogenides (TMDCs) with unique spin-valley contrasting properties and remarkably strong excitonic effects continue to be a subject of intense research interests. These model 2D semiconductors feature two fundamental intravalley excitons species–optically accessible 'bright' excitons with anti-parallel spins and optically inactive 'dark' excitons with parallel spins. For applications exploiting radiative recombination of bright excitons or long lifetime dark excitons, it is essential to understand the radiative character of the exciton ground state and establish the energy separation between the lowest energy bright and dark excitons. Here, we report a direct spectroscopic measure of dark excitons in monolayer $MoSe_2$ encapsulated in hexagonal boron nitride. By applying strong in-plane magnetic field, we induce mixing and splitting of bright and dark exciton branches, which enables an accurate spectroscopic determination of their energies. We confirm the bright character of the exciton ground state separated by a 1.5 meV gap from the higher energy dark exciton state, much smaller compared to the previous theoretical expectations. These findings provide critical information for further improvement of the accurate theoretical description of TMDCs electronic structure.

1. Introduction

Transition metal dichalcogenides (TMDCs) with the chemical formula MX_2, where M is a group IV–VII transition metal and X is a chalcogen atom (S, Se, Te), have recently emerged as a new class of layered materials that can be exfoliated down to atomically thin layers. Among these materials, the group VI (Mo, W) TMDC monolayers stand out due to their peculiar spin-valley coupled band structure with spin-polarized conduction and valence band states located at the band edges at the corners of the hexagonal Brillouin zone (K+ and K− valleys) with a direct gap in the visible or near-infrared region [1–3]. Because of time reversal symmetry, the sign of the spin splitting is opposite in K+ and K− valley. This allows one to address the spin-valley degree of freedom with either left or right circularly polarized light [4, 5] and, together with the strong excitonic effects, create a unique platform to study both light-matter interactions and spin-valley physics in the real two-dimensional (2D) limit [6–8].

Since allowed interband optical transitions must conserve the spin and the momentum, the optically active or bright exciton involves an electron and a hole belonging to the same valley but with opposite spins (the spin of the hole is opposite to that of the electron residing in the same valence band). Radiative recombination of intarvalley excitons with the electron and hole constituents with same spins is forbidden and such exciton states are called dark. The understanding

of the interplay between low energy bright and dark exciton states is of particular importance since these states ultimately define the radiative properties of 2D TMDCs and their relevance for applications in optoelectronics and valleytronics. In WSe_2 and WS_2 monolayers, the dark character of the ground state exciton and the energy separation between dark and higher energy bright excitons are firmly established both experimentally and theoretically [9–16]. Despite some recent efforts [10, 17], unambiguous experimental observation of low energy dark excitons in Mo-based compounds remains elusive, and recent theoretical studies have not always been consistent in predicting the energy of dark excitons and even whether Mo-based TMDCs host dark or bright lowest energy excitons [18–22].

In this letter, we present the first measurement of the dark exciton in monolayer $MoSe_2$. The main obstacles to detecting dark excitons in $MoSe_2$ are the very close separation between the bright and the higher energy dark states and the low population of the dark exciton states [12]. Due to recent progress in the fabrication of high quality BN encapsulated TMDC monolayers, it has become possible to prepare TMDC monolayers with very narrow exciton lines of about 1 meV FWHM [23]. With the aid of a strong in-plane magnetic field, we mix bright and dark exciton states, brighten dark excitons, induce further separation of bright and dark exciton states and successfully detect the elusive dark excitons in photoluminescence (PL) and reflectance contrast (RC) spectra. These experimental results provide an unambiguous evidence of the bright nature of exciton ground state in $MoSe_2$ as well as the accurate measure of the energy splitting between the lowest energy bright and dark excitons.

2. Magnetic field induced splitting of bright and dark excitons in monolayer TMDCs

Within a simple single particle picture, the radiative character, dark or bright, of intravalley excitons in monolayer TMDCs depends on the ordering of the spin-up and spin-down conduction sub-bands, CB↑ and CB↓, separated by a relatively small single-particle gap Δ_{CB} of the order of tens of meV [24]. For the valence states, only the higher energy spin-subband VB↑ needs to be considered because of the large, hundreds of meV, spin splitting in the valence band [25]. The relative ordering of lowest energy conduction subbands in MX_2 monolayers, which are formed mostly by d_{z^2} orbitals of transition metal atoms [26], is different for Mo- and W-based TMDCs. In molybdenum compounds, the lowest conduction band and the highest valence band share the same spin projection, so the lowest energy exciton state is expected to be optically active. However, the actual energy separation between the lowest energy bright and dark excitons states, Δ_{db}, has additional contributions from the short-range electron-hole exchange interaction as well as enhanced binding energy of dark excitons due to their heavier mass compared with bright excitons (see the theory section in the Supporting Information) [20, 21].

In order to access the dark exciton states, we apply an in-plane magnetic field $B_{\|}$ (B_x,B_y) to separate more dark (X^d) and bright (X^b) excitons and brighten otherwise unaccessible dark excitons. This is illustrated in figure 1(a) where we show a cartoon of the dispersion relation of excitons as a function of the exciton center-of-mass wavevector (Q). Only excitons located within the photon dispersion cone are allowed to recombine radiatively. The in-plane magnetic field does not couple to the orbital motion of the electrons and can effectively perturb the spin magnetic momenta of band electrons only. The effect of $B_{//}$ on the spin orientation of valence band electrons is negligible because of the large separation of spin–orbit split valence bands. Thus, the system can be approximated by a two-level Hamiltonian for bright and dark exciton states (see the theory section in the Supporting Information):

$$H_{\text{eff}} = \begin{pmatrix} E_b & \frac{1}{2}g_{cb}\mu_B B_{\|} \\ \frac{1}{2}g_{cb}\mu_B B_{\|} & E_d \end{pmatrix} \quad (1)$$

where E_b and $E_d = E_b + \Delta_{db}$ refer to the energies of the bright and dark states at zero magnetic field, the off-diagonal terms introduce their field-induced coupling, g_{cb} is the in-plane conduction band g-factor and μ_B is the Bohr magneton. $B_{\|}$ shifts the energies of bright and dark excitons in opposite directions:

$$E_{b,d}(B_{\|}) = (\Delta_{db} \mp \sqrt{{\Delta_{db}}^2 + {g_{cb}\mu_B B_{\|}}^2})/2 \quad (2)$$

where the plus/minus sign applies to the bright/dark exciton branches. Here we set $E_b(B = 0) = 0$ to consider in the following the energy shift of PL peaks versus magnetic field. $B_{\|}$ also provides small but finite optical oscillator strength, proportional to ${B_{\|}}^2$, for dark excitons. We note that despite its simplicity the two-level model has been proven to describe the behavior of brightened dark excitons remarkably well as, for example, in tungsten-based monolayer TMDCs [9, 10] or in carbon nanotubes [27, 28].

Magnetic brightening of dark excitons has been observed in tungsten-based TMDCs [9, 10], where the gap between bright and dark excitons is relatively large, ~50 meV. However, the actual field induced splitting between the bright and dark excitons has not been detected. From equation (2) we expect the change of exciton energies at the highest applied magnetic fields (31 T) to only be about (55–75) μeV for WS_2 or WSe_2, almost impossible to detect by standard methods. In contrast, since the field induced splitting is inversely proportional to the zero-field Δ_{db} (in the weak-field approximation), it is expected to be much stronger in $MoSe_2$, eventually reaching the meV scale at 20–30 T.

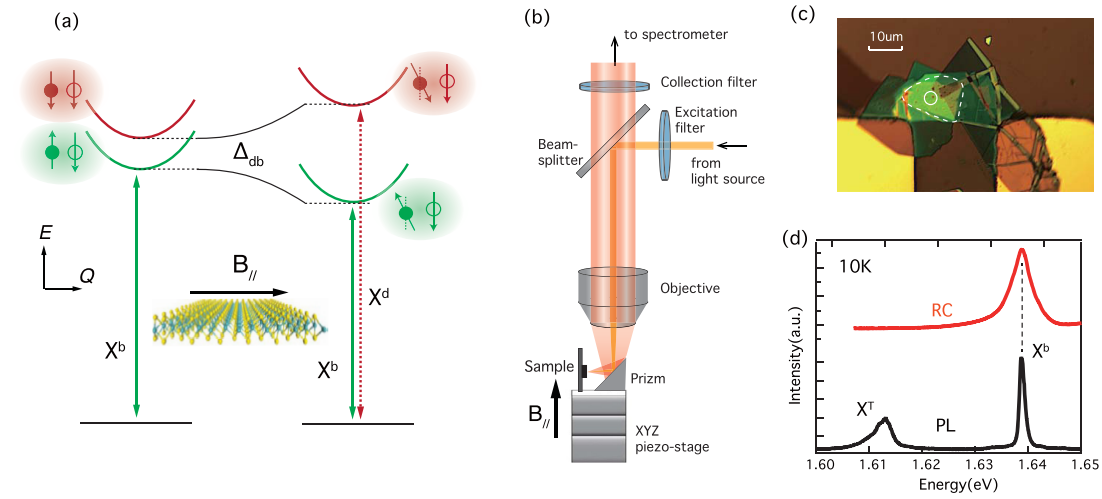

Figure 1. (a) Electronic dispersion of spin-allowed bright (X^b, depicted in green cartoons) and spin-forbidden dark (X^d, depicted in red cartoons) intravalley excitons in monolayer $MoSe_2$. The solid and open circles represent CB electrons and VB holes, respectively. The arrows illustrate the spin orientation. The spin orientation of a VB hole is opposite to that of a VB electron. The in-plane magnetic field mixes spin components of CB electrons, which transfer some oscillator strength from bright excitons to dark ones and further separate them in energy. In the experiment, this mechanism can be probed via magneto-optical spectroscopy in the Voigt configuration. (b) Schematics of the experimental setup for magneto-PL and magneto-reflectance measurements in the Voigt geometry. (c) The microscope image of the hBN encapsulated $MoSe_2$ device. The dashed line encloses the $MoSe_2$ monolayer. The excitation light spot is approximately indicated by the center circle. (d) PL and broadband RC spectra measured at 10 K. The bright neutral exciton (X^b) is observed in both PL and RC spectra. The PL emission at 26 meV below the neutral exciton peak is attributed to the trion (X^T) emission.

3. Results and discussion

Fabricating high quality $MoSe_2$ monolayers with narrow PL linewidth of about 1 meV is a crucial factor for detecting the exciton fine structure. Our samples were prepared by mechanical exfoliation of CVT or flux grown bulk $MoSe_2$ single crystals, then transferred and encapsulated in hexagonal boron nitride (hBN). A piece of few-layer graphene was used as the contact electrode of the single layer $MoSe_2$ and another piece was used as the transparent top-gate electrode on the top layer BN. The typical size of the monolayer $MoSe_2$ is about 10 ×10 μm^2 (figure 1(c)). Our hBN encapsulated samples exhibit very narrow exciton emission PL peaks (with FWHM as low as ∼1.1 meV at 10 K) approaching the intrinsic limit [23].

Low temperature magneto-spectroscopy measurements were carried out in the Voigt geometry (light wavevector perpendicular to B) with custom micro-spectroscopy setups equipped with a nonmagnetic objective and a three-axis piezostage for fine *in situ* positioning as illustrated in figure 1(b). The PL measurements were performed with a 31 T resistive magnet using excitation by a continuous-wave laser with a photon energy 2.41 eV (514 nm wavelength). To measure the reflectance contrast (RC), $\Delta R/R = (R_{\text{sample}} - R_{\text{substrate}})/R_{\text{substrate}}$, we employed a similar setup coupled to a 17.5 T superconducting magnet and used a Hg arc lamp with a combination of appropriate bandpath filters to define the spectral region of interest. The excitation light was focused by an objective (NA= 0.5) to a spot size of ∼2 μm. The excitation power delivered to the sample was 1 μW or less to avoid sample heating and minimize light-induced doping. The PL emission or reflected light was collected by the same objective and detected by a spectrometer equipped with a TE cooled CCD camera. The presented spectra were collected at 10 K and recorded with a spectral resolution of 0.11 meV. Characteristic zero field spectra of the monolayer $MoSe_2$ are shown figure 1(d). In accordance with prior studies, we observe strong and narrow PL emission line for neutral bright exciton (X^b) at 1.6388 eV and PL signal from charged excitons or trions (X^T) at 1.613 eV. The RC spectrum shows only one pronounced peak associated with X^b.

To show the effect of the in-plane magnetic field on exciton emission, we plot in figure 2(a) the 2D color map of PL intensity as a function of magnetic field from 0 T to 31 T. As $B_{||}$ increases, the X^b is redshifted and an additional peak, labelled as X^d, emerges on the higher energy of X^b side exhibiting a blueshift. At the highest magnetic field of 31 T, X^b shifts by 1.1 meV and the separation between two peaks, X^b and X^d, reaches approximately 4 meV. It is instructive to note that these observations provide an explanation for the results from our earlier attempts to detect field induced bright-dark excitons splitting in the PL spectra from $MoSe_2$ monolayers on SiO_2/Si substrates. Because the exciton PL line was relatively broad, FWHM = 7.3 meV, the Δ_{db} splitting could not be resolved spectroscopically even at $B_{||}$ = 31 T. However, as illustrated in supplementary figure S1 (stacks.iop.org/TDM/7/015017/mmedia), the field dependent behavior of the exciton PL peak measured on Si/SiO_2 $MoSe_2$ (0.8 meV red shift and 3 meV broadening) agrees well with the the actual split-

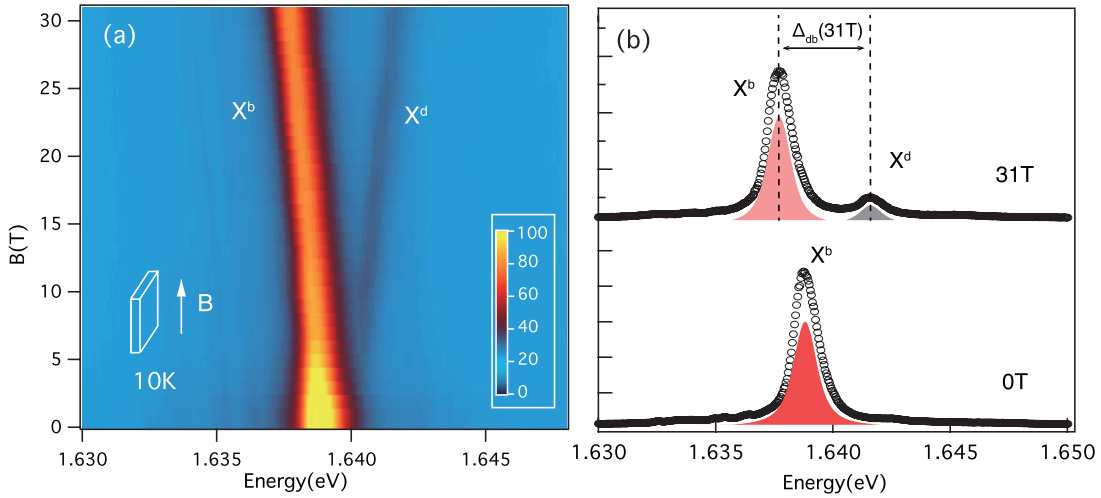

Figure 2. (a) Color map of the evolution of PL spectral intensity as a function of the in-plane magnetic field. The spectra were measured on the hBN encapsulated monolayer $MoSe_2$ in the intrinsic regime. (b) Comparison of the PL spectra (open circles) measured at zero magnetic field and at $B_{||} = 31$ T. The PL emission energies of $X^b(0T) = 1.6388$ eV, $X^b(31T) = 1.6377$ eV, $X^d(31T) = 1.6416$ eV, were determined from best peak fits (colored areas).

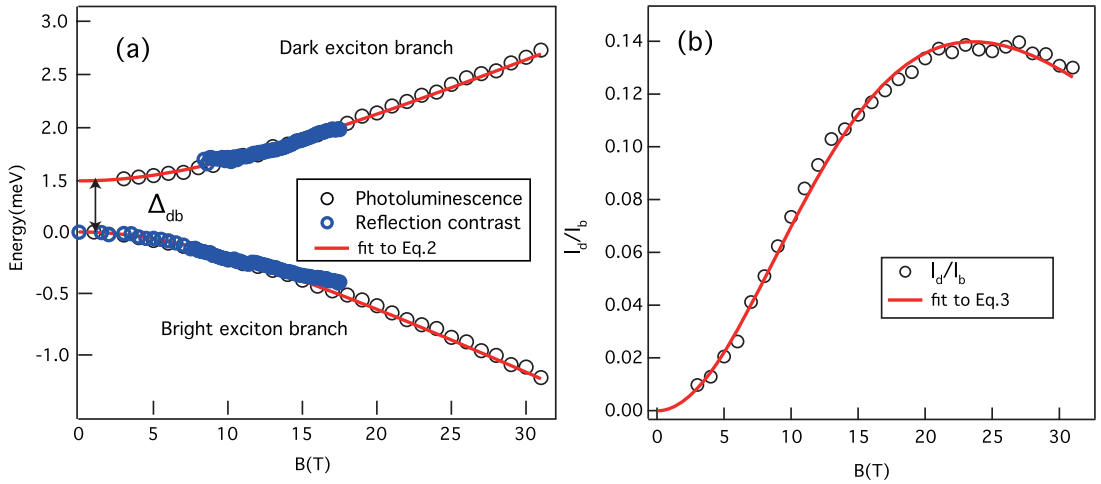

Figure 3. (a) Energy of dark and bright excitons as a function of $B_{||}$ extracted from PL and RC spectra. Solid lines are fits to equation (2). (b) Relative intensity of dark and bright excitons, $I_d/I_b(B_{||})$. Solid line represents the fit to equation (3).

ting of the bright and dark exciton resolved in PL and RC spectra from hBN encapsulated $MoSe_2$.

Since the observed behavior reflects very well the anticipated brightening of the dark exciton and field induced energy shift of bright and dark excitons in opposite directions, the emerging high energy peak is attributed to the magnetically brightened dark exciton. For a quantitative analysis of PL evolution with $B_{||}$, we use a pseudo-Voigt line shape to fit the spectra. The resulting overall change of X^b and X^d energies is plotted in figure 3(a). To ensure the reliability and consistency of the experiment and analysis, we also plot the exciton energies extracted from the RC spectra measured in fields up to 17.5 T (detailed comparison of PL and RC spectra is presented in supplementary figure S1). Both data sets consistently overlap, ensuring the validity of the PL results at higher magnetic fields.

As expected from the two band model, the energy of the bright (dark) exciton first exhibits a quadratic increase (decrease) followed by a linear dependence in the high field limit. Despite its simplicity, the model provides a facile means for accurate measure of the dark exciton energy at zero magnetic field and the g-factor. By fitting the measured $E_b(B_{||})$ and $E_d(B_{||})$ (see figure 3(a)) we extract a g-factor of 2.0 ± 0.1. This confirms the assumption that $B_{||}$ acts through mixing spins of the conduction band electrons, and the orbital or valence band contributions are negligible. For the zero-field dark exciton, we obtain $E_d = 1.6403$ eV, which places it above the bright state by just $\Delta_{db} = 1.5$ meV. This result represents the first unequivocal experimental observation of dark excitons in monolayer $MoSe_2$ and provides a clear evidence that the exciton ground state in this system is optically bright. Time-resolved PL experiments are expected to reveal longer radiative lifetime of the dark excitons [9, 13]. However, the separation of PL peaks in $MoSe_2$ is too small and PL emission from the higher energy brightened dark

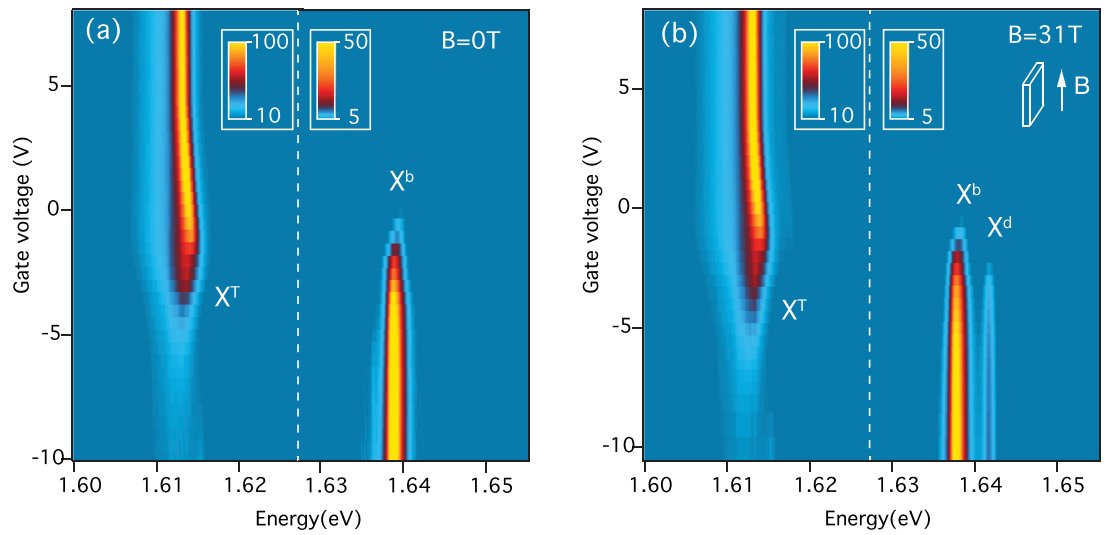

Figure 4. Gate dependence map of the PL intensity at 0 T (a) and $B_{\|} = 31$ T (b) and at $T = 10$ K. The intensity is plotted on a linear scale on the left sub-panels at energies below 1.6275 eV (indicated by dashed white line). The log scale with smaller range is used to enhance visibility on the right sub-panels (above 1.6275 eV). X^b and X^d represent bright and dark excitons. X^T is the negatively charged exciton (trion).

exciton is too weak for meaningful time-resolved PL measurements at high magnetic fields.

The energy splitting between the bright and dark excitons at the light cone, $\Delta_{db} = \Delta_{CB} + \Delta_x + \Delta_M$, has contributions from spin–orbit coupling energy splitting of the conduction band (Δ_{CB}), short range electron-hole exchange (Δ_x), and the fact that dark and bright excitons have different masses and therefore different binding energies (Δ_M). To compare the experimental value of Δ_{db} with theory, one has to accurately calculate the values of Δ_{CB}, Δ_x and Δ_M. To date, such a comparison is ineffective because the variation in reported *ab initio* calculations of these parameters is often larger than 10 meV [9, 20, 21, 29], i.e. larger than our measured value of Δ_{DB} in monolayer $MoSe_2$. Nonetheless, we can still make few consistent observations. Firstly, we note that $\Delta_x < 0$ due to the repulsive nature of the short-range exchange [9, 20, 21], and $\Delta_M < 0$ because dark excitons are heavier than bright ones (dark excitons involve the conduction band with heavier effective mass). Accordingly, to offset the negative value contributions of $\Delta_x + \Delta_M$, the value of Δ_{CB} should be positive in monolayer $MoSe_2$ in order to yield $\Delta_{db} = 1.5$ meV. Similarly, assuming that $\Delta_x + \Delta_M$ has similar magnitude in Mo- and W-based compounds, the value of Δ_{CB} should be negative in WSe_2 and WS_2 monolayers in order to yield $\Delta_{db} = -40$ meV and -55 meV, respectively [12]. Next, following the procedure described in the Supporting Information, we evaluate the binding energies of bright and dark excitons and obtain $\Delta_M = -8$ meV in $MoSe_2$ and ~ -16 meV in WSe_2. Assuming $\Delta_x \sim -10$ meV [9, 20], we can further infer that Δ_{CB} is in the ballpark of $+20$ meV in monolayer $MoSe_2$ and -20 meV in monolayer WSe_2. The latter is consistent with the measured value reported in [9]. We note that in addition to the contribution from spin–orbit coupling, the value of Δ_{CB} is affected from bandgap renormalization in electron-doped samples due to many-body exchange interactions [30, 31]. The experimental results and the analysis we have provided in this paper deal with intrinsic (un-doped) monolayers.

We now discuss the relative intensities of the PL emission of dark and bright excitons, I_d/I_b that we plot as a function of $B_{\|}$ in figure 3(b). At low magnetic fields, the dark exciton emission grows quadratically with $B_{\|}$, which is in agreement with the predictions of the two-band model, $I_d \propto I_b B_{\|}^2$, and previous observations in W-based monolayer TMDCs [9, 10, 16]. However, we find that in $MoSe_2$, the ratio of PL intensities I_d/I_b deviates from the simple quadratic dependence at magnetic fields above 7–10 T, saturates at higher fields and starts decreasing above 25 T (figure 3(b)). To understand this behavior, we have to consider changes in the thermal population of X^d. Since the bright exciton is the ground excitonic state and the separation between bright and dark states increases with $B_{\|}$, the population of the high-lying dark state becomes thermally suppressed as magnetic field increases. Assuming thermal equilibrium occupation numbers, we modify the expression for the relative intensity by adding a Boltzmann factor:

$$I_d \propto I_b {B_{\|}}^2 e^{\frac{-\Delta_{db}(B_{\|})}{k_B T}}, \qquad (3)$$

which results in excellent fit to the experimental data (figure 3(b)).

Finally, we briefly discuss another possible mechanism, the Bychkov–Rashba effect [32], that may flip the spin of the conduction band electrons and contribute to brightening of the dark exciton. The Bychkov–Rashba type coupling between dark and bright intraband excitons would require breaking the mirror symmetry in respect to the monolayer plane, which could be induced, for example, by out-of-plane

electric field generated by a gate or by unintentional, impurity related charge of the substrate [19, 33]. To examine this possibility, we perform gate dependent PL measurements. Figure 4(a) shows a color map of the PL spectrum of the device at zero magnetic field as a function of the top gate voltage. In the whole wide range of applied gate voltages, only two PL peaks are observed related to neutral bright exciton emission (X^b) and charged exciton emission (X^T). No signatures of the PL emission on the higher energy side of X^b can be detected in the spectra acquired at $B = 0$ T. The gate dependent PL measured at $B_{\|} = 31$ T (figure 4(b)) clearly reveals a signal associated with the emission from dark excitons, X^d, situated at approximately 4 meV above X^b. The energy separation and relative intensities are nearly independent on the gate voltage, and, consistent with theoretical estimations, indicates that the electric field does not contribute to the brightening of dark excitons. Even at relatively high electric field of 1 V nm^{-1}, the resulting radiative rate for dark excitons is expected to be four orders of magnitude smaller compared to the effect of of an applied in-plane magnetic field of 30 T [33]. The negligible role of the Rashba-induced mixing between dark and bright excitons in our experiment is corroborated by the fact that this interaction is proportional to the exciton wavevector Q (see the Supporting Information), and therefore its effect vanishes within the light cone wherein $Q \to 0$.

4. Conclusions

In conclusion, we have observed magnetic field induced brightening of the dark exciton and splitting of bright and dark neutral excitons in high quality monolayer h-BN encapsulated $MoSe_2$. The superior sample quality and the use of a strong in-plane magnetic field enable a direct spectroscopic probe of dark excitons. We have confirmed that the lowest energy exciton state is optically active. The energy separation between the ground state bright exciton and higher energy dark exciton is determined to be 1.5 meV. This result implies that the energy splitting in the conduction band is a few tens of meV in order to offset the reduced binding energy of bright excitons due to the repulsive short-range electron-hole exchange as well as their lighter mass compared with dark excitons. Importantly, our findings demonstrate that the bright and dark exciton branches are nearly degenerate, and this result may be intimately related to the enhanced valley depolarization in monolayer $MoSe_2$ [34–36].

Acknowledgments

This work was primarily supported by the Department of Energy, Basic Energy Sciences, under Contract No. DE- FG02-07ER46451. The $MoSe_2$ crystal growth and the sample fabrication at Columbia University were supported by by the NSF MRSEC program through Columbia in the Center for Precision Assembly of Superstratic and Superatomic Solids (DMR-1420634). The device fabrication at Rensselaer Polytechnic Institute (RPI) was supported by the NY State Empire State Development's Division of Science, Technology, and Innovation (NYSTAR) through Focus Center-NYRPI Contract C150117. Z Li acknowledges support from the Shanghai Sailing Program (19YF1425200). S-F Shi acknowledges support by AFOSR through Grant FA9550-18-1-0312. The experiments were performed at the National High Magnetic Field Laboratory (NHMFL), which is supported by NSF Cooperative Agreement DMR-1157490, DMR-1644779 and the State of Florida. The work at the University of Rochester was supported by the Department of Energy, Basic Energy Sciences, under Contract No. DE-SC0014349.

ORCID iDs

Dinh Van Tuan https://orcid.org/0000-0002-9605-2686
Zhigang Jiang https://orcid.org/0000-0001-9884-3337
Su-Fei Shi https://orcid.org/0000-0001-5158-805X
Hanan Dery https://orcid.org/0000-0002-2640-4068
Dmitry Smirnov https://orcid.org/0000-0001-6358-3221

References

[1] Mak K F, Lee C, Hone J, Shan J and Heinz T F 2010 Atomically thin MoS_2: a new direct-gap semiconductor *Phys. Rev. Lett.* **105** 136805
[2] Splendiani A *et al* 2010 Emerging photoluminescence in monolayer MoS_2 *Nano Lett.* **10** 1271
[3] Xiao D, Liu G-B, Feng W, Xu X and Yao W 2012 Coupled spin and valley physics in monolayers of MoS_2 and other group-VI dichalcogenides *Phys. Rev. Lett.* **108** 196802
[4] Mak K F, He K, Shan J and Heinz T F 2012 Control of valley polarization in monolayer MoS_2 by optical helicity *Nat. Nanotechnol.* **7** 494
[5] Cao T *et al* 2012 Valley-selective circular dichroism of monolayer molybdenum disulphide *Nat. Commun.* **3** 887
[6] Yu H, Cui X, Xu X and Yao W 2015 Valley excitons in two-dimensional semiconductors *Natl Sci. Rev.* **2** 57
[7] Koperski M *et al* 2017 Optical properties of atomically thin transition metal dichalcogenides: observations and puzzles *Nanophotonics* **6** 1289
[8] Wang G *et al* 2018 Colloquium: Excitons in atomically thin transition metal dichalcogenides *Rev. Mod. Phys.* **90** 021001
[9] Zhang X-X *et al* 2017 Magnetic brightening and control of dark excitons in monolayer WSe_2 *Nat. Nanotechnol.* **12** 883
[10] Molas M R *et al* 2017 Brightening of dark excitons in monolayers of semiconducting transition metal dichalcogenides *2D Mater.* **4** 021003
[11] Zhou Y *et al* 2017 Probing dark excitons in atomically thin semiconductors via near-field coupling to surface plasmon polaritons *Nat. Nanotechnol.* **12** 856
[12] Wang G *et al* 2017 In-Plane propagation of light in transition metal dichalcogenide monolayers: optical selection rules *Phys. Rev. Lett.* **119** 047401
[13] Robert C, Amand T, Cadiz F, Lagarde D, Courtade E, Manca M, Taniguchi T, Watanabe K, Urbaszek B and Marie X 2017 Fine

structure and lifetime of dark excitons in transition metal dichalcogenide monolayers *Phys. Rev.* B **96** 155423
[14] Vasconcelos R, Braganca H, Qu F and Fu J 2018 Dark exciton brightening and its engaged valley dynamics in monolayer WSe_2 *Phys. Rev.* B **98** 195302
[15] Park K-D, Jiang T, Clark G, Xu X and Raschke M B 2018 Radiative control of dark excitons at room temperature by nano-optical antenna-tip Purcell effect *Nat. Nanotechnol.* **13** 59
[16] Molas M R *et al* 2019 Probing and manipulating valley coherence of dark excitons in monolayer WSe_2 *Phys. Rev. Lett.* **123** 096803
[17] Quereda J, Ghiasi T S, van Zwol F A, van der Wal C H and van Wees B J 2018 Observation of bright and dark exciton transitions in monolayer $MoSe_2$ by photocurrent spectroscopy *2D Mater.* **5** 015004
[18] Palummo M, Bernardi M and Grossman J C 2015 Exciton radiative lifetimes in two-dimensional transition metal dichalcogenides *Nano Lett.* **15** 2794–800
[19] Dery H and Song Y 2015 Polarization analysis of excitons in monolayer and bilayer transition-metal dichalcogenides *Phys. Rev.* B **92** 125431
[20] Echeverry J P, Urbaszek B, Amand T, Marie X and Gerber I C 2016 Splitting between bright and bark excitons in bransition betal dichalcogenide monolayers *Phys. Rev.* B **93** 121107
[21] Deilmann T and Thygesen K S 2017 Dark excitations in monolayer transition metal dichalcogenides *Phys. Rev.* B **96** 201113
[22] Malic E *et al* 2018 Dark excitons in transition metal dichalcogenides *Phys. Rev. Mater.* **2** 014002
[23] Ajayi O A *et al* 2017 Approaching the intrinsic photoluminescence linewidth in transition metal dichalcogenide monolayers *2D Mater.* **4** 031011
[24] Kośmider K, González J W and Fernández-Rossier J 2013 Large spin splitting in the conduction band of transition metal dichalcogenide monolayers *Phys. Rev.* B **88** 245436
[25] Zhu Z Y, Cheng Y C and Schwingenschlögl U 2011 Giant spin-orbit-induced spin splitting in two-dimensional transition-metal dichalcogenide semiconductors *Phys. Rev.* B **84** 153402
[26] Liu G-B, Shan W-Y, Yao Y, Yao W and Xiao D 2013 Three-band tight-binding model for monolayers of group-VIB transition metal dichalcogenides *Phys. Rev.* B **88** 085433
[27] Shaver J, Crooker S A, Fagan J A, Hobbie E K, Ubrig N, Portugall O, Perebeinos V, Avouris Ph and Kono J 2008 Magneto-optical spectroscopy of highly aligned carbon nanotubes: identifying the role of threading magnetic flux *Phys. Rev.* B **78** 081402
[28] Srivastava A, Htoon H, Klimov V I and Kono J 2008 Direct observation of dark excitons in individual carbon nanotubes: inhomogeneity in the exchange splitting *Phys. Rev. Lett.* **101** 087402
[29] Kormányos A, Burkard G, Gmitra M, Fabian J, Zólyomi V, Drummond N D and Fal'ko V 2015 $\mathbf{k}\cdot\mathbf{p}$ theory for two-dimensional transition metal dichalcogenide semiconductors *2D Mater.* **2** 022001
[30] Scharf B, Van Tuan D, Zutic I and Dery H 2019 Dynamical screening in monolayer transition-metal dichalcogenides and its manifestations in the exciton spectrum *J. Phys.: Condens. Matter* **31** 203001
[31] Van Tuan D, Scharf B, Wang Z, Shan J, Mak K F, Zutic I and Dery H 2019 Probing many-body interactions in monolayer transition-metal dichalcogenides *Phys. Rev.* B **99** 085301
[32] Bychkov Yu A and Rashba E I 1984 Properties of a 2D electron gas with lifted spectral degeneracy *J. Exp. Theor. Phys. Lett.* **39** 78
Bychkov Yu A and Rashba E I 1984 *Pis'ma Zh. Eksp. Teor. Fiz.* **39** 66
[33] Slobodeniuk A O and Basko D M 2016 Spinflip processes and radiative decay of dark intravalley excitons in transition metal dichalcogenide monolayers *2D Mater.* **3** 035009
[34] Wang G, Palleau E, Amand T, Tongay S, Marie X and Urbaszek B 2015 Polarization and time-resolved photoluminescence spectroscopy of excitons in $MoSe_2$ monolayers *Appl. Phys. Lett.* **106** 112101
[35] Kioseoglou G, Hanbicki A T, Currie M, Friedman A L and Jonker B T 2016 Optical polarization and intervalley scattering in single layers of MoS_2 and $MoSe_2$ *Sci. Rep.* **6** 25041
[36] Tornatzky H, Kaulitz A-M and Maultzsch J 2018 Resonance profiles of valley polarization in single-layer MoS_2 and $MoSe_2$ *Phys. Rev. Lett.* **121** 167401